Journal of Food Science and Technology (Iran)

Homepage:www.fsct.modares.ir

Scientific Research

Optimizing the Electrospinning Process of Poly vinyl alcohol-Based Nanocarriers Containing Microwave-Roasted Camelina (*Camelina sativa* L.) Seed Oil

Sanaz Khaledi[1], Nafiseh Jahanbakhshian[2*], Zahra Emam-Djomeh[3], Sediqeh Soleimanifard[4], Zahra Beigmohammadi[1]

1-Department of Food Science and Technology, NT.C., Islamic Azad University, Tehran, Iran
2-Department of Food Science and Technology, ShK.C., Islamic Azad University, Shahrekord, Iran
3-Transfer Phenomena Laboratory (TPL), Department of Food Science, Technology and Engineering, Faculty of Agricultural Engineering and Technology, University of Tehran, Karaj, Iran
4-Department of Food Science and Technology, Faculty of Agriculture, University of Zabol, Zabol, Iran

ARTICLE INFO

Article History:

Received: 2025/07/28

Review: 2025/09/30

Accepted: 2025/10/07

Keywords:

Nanocarrier,
Electrospinning,
Camelina oil,
Response surface methodology,
Roasted

DOI: **10.48311/fsct.2026.84077.0**

*Corresponding Author E-

njahanbakhshian@iau.ac.ir

ABSTRACT

Nanocarriers, as advanced delivery systems for bioactive compounds, play a pivotal role in enhancing stability, improving functionality, and enabling innovative applications in food and packaging industries. This study focuses on the fabrication and optimization of biocompatible nanocarriers based on poly(vinyl alcohol) (PVA) loaded with microwave-roasted *Camelina sativa* seed oil (CSO), aimed at applications in smart food packaging. Electrospinning combined with Response Surface Methodology (RSM) using a Central Composite Rotatable Design (CCRD) was employed to investigate the effects of key processing variables, including oil concentration (5–25% w/w), applied voltage (10–30 kV), tip-to-collector distance (7.5–22.5 cm), and pump rate (0.5–5 mL/h), on the nanocarrier diameter. The developed regression model showed a high degree of fit, confirming strong correlations between the factors and response (R^2=0.998). Analysis of variance and Pareto chart indicated that pump rate and CSO concentration significantly influenced fiber diameter. Increasing CSO concentration led to thicker and more uniform fibers, attributed to higher viscosity and reduced charge density. These nanocarriers offer controlled release of bioactive compounds and are promising candidates for use in active and intelligent food packaging systems.

1- Introduction

In recent decades, encapsulation has been recognized as one of the key technologies for protecting sensitive bioactive compounds, including vegetable oils, antioxidants, and essential oils, against environmental degradation factors such as light, oxygen, heat, and humidity [1]. This technology, by entrapping the target substance within a protective matrix, not only enhances its stability but also enables its controlled and targeted release under desirable conditions. In this regard, the development of nanocarrier systems with particle sizes at the nanometric scale has attracted particular attention due to their high specific surface area and suitable permeability [2, 3].

One of the novel and effective methods for producing nanocarriers is electrospinning technology. This technique, by applying a strong electric field, enables the production of polymeric fibers with nanometric diameters, porous structures, and high loading capacity for bioactive compounds [4]. Electrospun nanofibers, owing to their unique morphological and physical characteristics such as high specific surface area, controlled permeability, and compatibility with various compounds, are considered ideal candidates for encapsulation of sensitive substances [5]. However, achieving uniform and high-quality nanofibers requires precise optimization of process parameters such as polymer concentration, active compound loading ratio, applied voltage, nozzle-to-collector distance, and flow rate, especially when the encapsulated substance has an oily and nonpolar nature [6].

In this study, Camelina seed oil (*Camelina sativa* L.) was selected as the target bioactive compound. This oil, due to its richness in omega-3 (particularly alpha-linolenic acid) and omega-6 fatty acids, along with antioxidant compounds such as tocopherols, flavonoids, and phenolic compounds, possesses high potential for nutritional and functional applications [7-9]. However, its high susceptibility to oxidation—resulting from the unsaturated structure of its lipids—represents a major limitation for its direct use [10, 11].

To overcome this challenge, microwave roasting was employed as a pretreatment method for the oil in this study. This process, through rapid and volumetric heating, reduces processing time and enhances the release of bioactive compounds, particularly phenolic and antioxidant substances. Although heat distribution in microwave processing can be nonuniform, the volumetric nature of microwave heating offers significant advantages compared to conventional thermal methods [12, 13]. Furthermore, microwave roasting leads to viscosity adjustment, improved thermal stability, and reduced oxidation tendency of the oil—features that provide more suitable conditions for encapsulation and successful electrospinning. Therefore, the use of microwave-roasted Camelina oil, compared to raw oil, can improve loading efficiency, process stability, and the final quality of the nanofibers [1].

Poly(vinyl alcohol) (PVA) was selected as the polymeric matrix. This polymer, due to its biocompatibility, low toxicity, film-forming ability, and water solubility, is one of the most common polymers used in the formulation of electrospun nanocarriers [14, 15]. The combination of PVA with microwave-roasted Camelina oil creates a suitable system for the protection and controlled release of sensitive compounds. However, before

any application, precise optimization of the electrospinning process for this specific system is inevitable [14].

To achieve this goal, the Response Surface Methodology (RSM), as a powerful statistical tool, allows the simultaneous investigation of multiple process variables and their interactions with a minimal number of experiments [16]. The use of statistical design not only reduces experimental cost and time but also enables prediction of system behavior under various conditions and identification of the optimal operational point [17].

In this study, the main objective is to optimize the electrospinning process of PVA nanocarriers containing microwave-roasted CSO. Using RSM design and evaluating the morphological and structural properties of the produced nanofibers, the effect of key process variables on the quality of the final product will be investigated, and the optimal production conditions will be identified. Although these nanocarriers may later be applied in active packaging or similar fields, the present work is limited to the optimization of the production process and the physical–structural properties of the nanofibers. Accordingly, the novelty of this research lies in integrating a pretreated vegetable oil (microwave-roasted to enhance bioactive compounds) with PVA polymer in the electrospinning process and systematically optimizing it using a statistical RSM approach. The findings of this study can serve as a foundation for the future development of controlled-release systems in the food and pharmaceutical industries.

2- Materials and Methods

2.1. Materials

Camelina seeds were purchased from a retail store in Kermanshah Province, Iran. After manual purification, the seeds were stored in polypropylene bags and prepared for subsequent processing and analysis. PVA with a molecular weight of 115,000 was obtained from Sigma-Aldrich (USA). All other chemicals required for the experiments were purchased from Merck (Germany). All reagents were used without further purification.

2.2. Methods

2.2.1. Microwave Roasting of Seeds

For the thermal treatment and oil extraction of Camelina seeds, 4.55 g of seeds were roasted using a domestic microwave oven (Butane, Iran) operating at a frequency of 2450 MHz. The seeds were placed in a glass Petri dish with an approximate diameter of 10 cm and exposed to microwave irradiation at 450 W for 926 seconds. After the microwave treatment, the seeds were allowed to cool to room temperature. All chemical analyses, including oil content, free fatty acid content, peroxide value, and oxidative stability index, were performed according to the official methods of the American Oil Chemists' Society (AOCS) [1].

2.2.2. Oil Extraction

Oil extraction was performed using the Soxhlet method. For this purpose, 10 g of ground Camelina seeds were packed in filter paper and placed in the extraction chamber of the apparatus. Then, 75 mL of hexane was added to the device to allow a complete siphon cycle. After initiating the condenser and adjusting the cooling water flow, extraction was continued for 3 h at the boiling point of the solvent. Upon

completion, the filter paper contents were dried and reweighed to calculate the extracted oil yield [18].

2.2.3. Electrospinning of Nanocarriers

PVA (10% w/v) was dissolved in distilled water at 80 °C for 4 h and subsequently stirred continuously for 24 h at 25 °C to ensure complete hydration [19]. CSO was added to the PVA solution and homogenized using an ultrasonic probe device (Hielscher, Germany) for 5 minutes. Electrospinning was performed using a horizontal setup operated at 25 ± 1 °C and a relative humidity of 30–35%. The system consisted of a syringe pump (Terumo, Japan) with a feed rate of 0.01–10 mL/h, a 1 mL syringe fitted with a 21-gauge needle, and a high-voltage power supply (input: 220 V AC; output: 30 kV DC). The positive electrode was connected to the needle tip, while an aluminum foil attached to a rotating cylindrical collector served as the grounded (negative) electrode.

2.2.4. Optimization of Electrospinning Conditions

To produce PVA nanocarriers containing microwave-roasted CSO, four independent variables—oil content, pump speed, needle-to-collector distance, and applied voltage—were investigated to determine the optimal nanocarrier diameter using RSM based on a Central Composite Rotatable Design (CCRD). A second-order polynomial equation was fitted to express the relationship between independent and dependent variables and to establish their correlations. Table 1 presents the coded levels of the electrospinning parameters for nanocarrier preparation. The average nanocarrier diameter (in nanometers) was selected as the response variable.

Table 1. Actual and coded values of variables based on central composite design of PVA-CSO nanocarrier

Variable/Level	-α	-1	0	+1	+α
CSO concentration (%wt.)	5	10	15	20	25
Pump rate (mL/h)	0.5	1.625	2.75	3.875	5
Distanse between needle tip and collector (cm)	7.5	11.25	15	18.75	22.5
Applied voltage (kV)	10	15	20	25	30

2.2.5. Microstructure

To study the microstructure (morphology), images of the optimized nanocarrier were obtained using a scanning electron microscope (SEM). Prior to imaging, the samples were coated with a thin layer of gold, and then imaged using an acceleration voltage ranging from 15 to 30 kV at various magnifications. To determine the nanocarrier diameter, the SEM images were analyzed using ImageJ software. For this purpose, the average diameter of 10 randomly selected nanocarriers in each image was measured and analyzed [20].

2.3. Statistical Analysis

All statistical analyses were performed using OriginPro 2024, Microsoft Excel 2016, and Design-Expert v11 software. To optimize the process and evaluate the effects of independent variables, a CCRD based on the RSM was employed. The significance of the models and individual factor effects was evaluated using Analysis of Variance (ANOVA). A statistical significance level of $p < 0.05$ was considered, and all p-values related to model parameters and comparisons are reported in the results.

3-Results and Discussion

Table 2 presents the experimental design and the measured response for each experiment.

Table 2. RSM design of actual/coded factors and experimental response of PVA-CSO nanocarrier

Run	CSO concentration (%wt)	Pump rate (mL/h)	Distanse (cm)	Applied voltage (kV)	Diameter (nm)
1	15	2.75	15	20	426.1
2	15	0.5	15	20	557.4
3	20	1.625	11.25	15	505.8
4	10	1.625	18.75	25	454.8
5	10	3.875	18.75	15	563.2
6	15	2.75	15	20	422.9
7	15	2.75	15	20	424.8
8	15	2.75	7.5	20	473.3
9	10	1.625	11.25	15	475.7
10	20	1.625	11.25	25	492.9
11	20	1.625	18.75	15	491.3
12	10	1.625	11.25	25	468.1
13	20	3.875	11.25	25	557.4
14	20	3.875	18.75	25	546.5
15	10	1.625	18.75	15	452.6
16	15	2.75	22.5	20	445
17	15	5	15	20	726.2
18	15	2.75	15	20	427.7
19	10	3.875	11.25	15	591.6
20	20	3.875	18.75	15	608.2
21	15	2.75	15	20	435.9
22	20	1.625	18.75	25	495.4
23	25	2.75	15	20	510.1
24	15	2.75	15	20	428.2
25	15	2.75	15	10	534.3
26	5	2.75	15	20	447.6
27	10	3.875	11.25	25	545.4
28	20	3.875	11.25	15	618.3
29	15	2.75	15	30	481.6
30	10	3.875	18.75	25	508.3

The Pareto chart, presented in Fig 1, serves as a statistical tool for ranking and comparing the magnitude of the effects of independent variables on the response variable. This chart, by displaying the absolute values of the standardized effects of each factor and their interactions, provides a visual means to analyze the influence of each variable on the target response. Through this chart, it can be clearly identified which variables have dominant effects and which have lesser impacts on the response variations. The reference line in the Pareto chart also provides a criterion for determining the statistical significance of the effects (at a 95% confidence level), thereby facilitating the identification of influential factors.

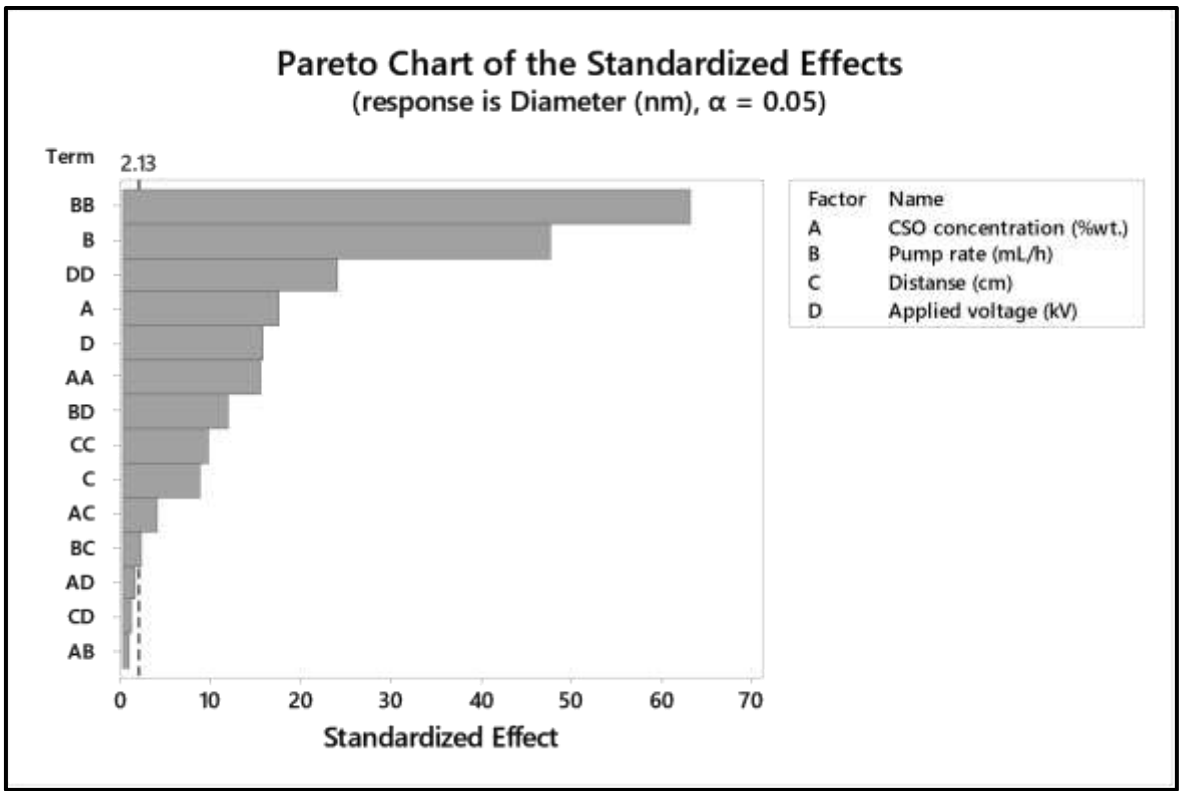

Fig 1. Pareto chart evaluating the effects of process variables on the diameter (nm) of PVA-CSO nanocarriers

The analysis of the results obtained from the Pareto chart (Fig 1), which serves as an effective tool for determining the significance of influential factors in statistical models, revealed that the quadratic term of pump speed (B^2) had the greatest contribution to the variation in the nanocarrier diameter. This finding indicates the nonlinear and significant role of pump speed in the formation process and dimensional control of electrospun fibers. On the other hand, the interaction between pump speed and the distance between the needle and collector (BC) showed the least effect among the evaluated factors, which may be attributed to the limited overlap of their individual influences and reduced synergistic interaction under the applied conditions. It is important to note that the Pareto chart, based on the absolute values of the standardized coefficients in the model, only illustrates the magnitude of each factor's or interaction's effect, without indicating its direction (positive or negative influence on the response variable) [21]. Therefore, a more comprehensive interpretation requires the examination of regression coefficients and response surface plots to identify the increasing or decreasing trends of the parameters. Furthermore, based on the comparison of coefficients with the reference line in the Pareto chart and the results of the ANOVA, it was found that, except for three interactions—Camelina oil content and applied voltage (AD), needle-to-collector distance and voltage (CD), and Camelina oil content and pump speed (AB)—all other main and interaction effects were statistically significant at a 95% confidence level. These findings highlight the critical

influence of process variables, particularly at nonlinear and interactive levels, in precisely controlling the morphology and final dimensions of nanofibers. The importance of this outcome lies in the design of targeted nanocarriers for controlled release of bioactive compounds, such as plant oils with high antioxidant activity, which can significantly enhance the performance of smart and active packaging systems in the food industry.

The effect of process parameters (oil content, applied voltage, pump speed, and needle-to-collector distance) on the nanocarrier diameter is illustrated in Fig 2.

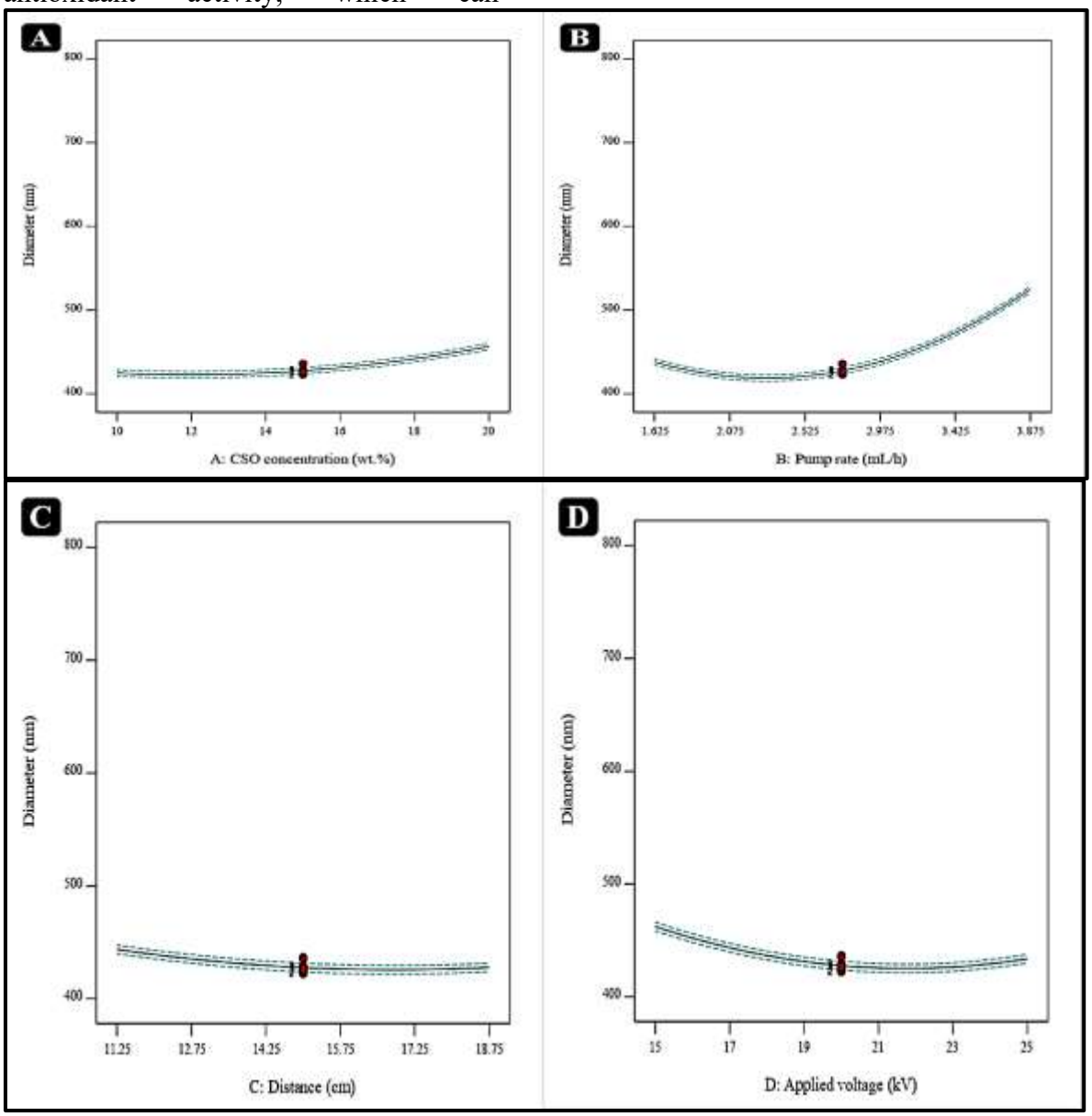

Fig 2. Independent effect of (A) CSO concentration (%wt.), (B) pump speed (mL/h), (C) distance (cm) and (D) applied voltage (kV) on the diameter (nm) of the PVA-CSO nanocarrier

The increase in nanocarrier diameter following the addition of CSO to the polymer solution is one of the key and multifactorial phenomena in the electrospinning process. In this process, the structural composition of the precursor solution plays a decisive role in determining the stretching behavior of the electrospinning jet and, consequently, the morphology and size of the resulting nanostructures [22]. The incorporation of CSO, which contains lipophilic and mostly nonionic compounds, leads to a reduction in the electrical conductivity of the solution. This decrease in conductivity corresponds to a lower number of free ions in the medium, directly reducing the charge density carried by the jet [23]. When the charge density decreases, the electrostatic stretching force exerted along the jet becomes significantly weaker. As a result, the elongation of polymer chains during the jet's flight from the needle to the collector becomes limited, and the thinning of the jet flow is restricted [24]. Consequently, the final nanocarrier structures are formed with larger diameters compared to those obtained without oil incorporation. Additionally, the increased viscosity of the polymer solution in the presence of CSO is another contributing factor to this diameter enlargement, since more viscous fluids resist elongation and thinning more strongly. Several studies have reported that the incorporation of oils or oil-based plant extracts directly influences the physical properties of electrospinning solutions [25]. These additives not only decrease electrical conductivity but also tend to increase both surface tension and viscosity, both of which reduce the efficiency of the electric field in stretching the polymer solution effectively [26]. Under such conditions, the resulting fibers typically exhibit thicker structures or, in some cases, form beads or droplets with larger dimensions instead of continuous fibers. Moreover, the presence of hydrophobic compounds in the spinning solution can influence solvent evaporation behavior. During electrospinning, rapid solvent evaporation during the jet flight promotes the formation of thin and stable structures [27]. However, the presence of a lipid phase may slow down the evaporation rate, allowing more time for molecular aggregation and the formation of denser, thicker structures [28]. Overall, it can be concluded that the addition of CSO affects not only the physical and electrical properties of the spinning solution but also the dynamic behavior of the jet under the electric field, thereby significantly influencing the morphology and dimensions of electrospun nanocarriers.

To evaluate the significance of the regression model and the effects of independent variables on the response (mean fiber diameter), an ANOVA was performed. The results of this analysis, presented in Table 3, demonstrate the goodness of fit of the model and the contribution of each variable and their interactions to the variation in the response.

Table 3. ANOVA for PVA-CSO nanocarrier Quadratic model

Source	Sum of Squares	df	Mean Square	F-value	p-value	
Model	1.451E+05	14	10365.43	522.64	< 0.0001	significant
A-CSO concentration (wt.%)	6051.55	1	6051.55	305.13	< 0.0001	
B-Pump rate (mL/h)	45058.00	1	45058.00	2271.88	< 0.0001	

C-Distance (cm)	1528.01	1	1528.01	77.04	< 0.0001	
D-Applied voltage (kV)	4910.62	1	4910.62	247.60	< 0.0001	
AB	9.46	1	9.46	0.4768	0.5004	
AC	296.70	1	296.70	14.96	0.0015	
AD	38.75	1	38.75	1.95	0.1825	
BC	90.73	1	90.73	4.57	0.0493	
BD	2743.14	1	2743.14	138.31	< 0.0001	
CD	18.71	1	18.71	0.9432	0.3469	
A^2	4683.84	1	4683.84	236.16	< 0.0001	
B^2	79405.73	1	79405.73	4003.73	< 0.0001	
C^2	1818.62	1	1818.62	91.70	< 0.0001	
D^2	11350.65	1	11350.65	572.31	< 0.0001	
Residual	297.49	15	19.83			
Lack of Fit	196.05	10	19.61	0.9664	0.5518	not significant
Pure Error	101.44	5	20.29			
Cor Total	1.454E+05	29				

The ANOVA results for the second-order model predicting the mean diameter of PVA-CSO nanocarriers indicated that the model is statistically significant (F-value = 522.64, $p < 0.0001$), with only a 0.01% probability that such a large F-value could be due to noise or random factors. All independent variables, including CSO content (A), pump speed (B), needle-to-collector distance (C), and applied voltage (D), were significant at $p < 0.0001$, demonstrating the independent and substantial influence of each parameter on the final fiber diameter. Among these variables, pump speed (B) exhibited the largest linear effect (F-value = 2271.88), whereas needle-to-collector distance (C) had the smallest linear effect (F-value = 77.04).

Among the two-factor interactions, only AC, BC, and BD were significant, while other interactions were not statistically significant, indicating that these variables mostly act independently. Additionally, all quadratic effects (A^2, B^2, C^2, and D^2) were significant at $p < 0.0001$, reflecting a strong nonlinear behavior of the variables on fiber diameter, particularly B^2 (F-value = 4003.73), which showed the most pronounced nonlinear effect. The Lack of Fit test indicated an F-value of 0.97 with $p = 0.5518$, confirming that the proposed model adequately describes the data without the need for more complex terms and can serve as an efficient tool for predicting and optimizing nanocarrier diameter in the PVA-CSO electrospinning process.

The fitted regression model demonstrated a very strong correlation between variables and response ($R^2 = 0.998$, adjusted $R^2 = 0.996$, predicted $R^2 = 0.991$), with a difference between R^2 and adjusted R^2 of less than 0.02, indicating the high validity of the model. The Adequate Precision value of 95.864 signifies an excellent signal-to-noise ratio (well above the minimum of 4), confirming the model's adequacy for exploring the design space. Furthermore, ANOVA results highlighted that pump speed and oil content have the most significant impact on nanocarrier diameter.

Two models can be proposed for these four variables based on the RSM. The derived equation in terms of coded factors provides a practical tool for predicting the response at various levels of independent variables. In this approach, actual factor values are converted to standardized coded values ranging from –1 to +1 to facilitate analysis and comparison of effects, where the low, middle, and high levels correspond to –1, 0, and +1, respectively. The main advantage of coding is that it allows direct comparison of factor coefficients, as the magnitude of each coefficient—after removing units and standardizing scales—indicates the relative influence of that factor on the response: the larger the coefficient, the more important the factor. Interaction terms in the equation reveal the combined effects of factors, and their coefficients indicate the magnitude of these combined effects. Therefore, this equation not only serves for response prediction but also provides a deeper understanding of system behavior and identification of key factors and their interactions during the process [29].

Final Equation of Diameter (nm) in Terms of Coded Factors = +427.60 +15.88A +43.33B -7.98C -14.30D +4.31AC -2.38BC -13.09BD +13.07A^2 +53.81B^2 +8.14C^2 +20.34D^2

The equation expressed in terms of actual factors provides a practical tool for predicting the system response under real physical conditions of the variables, enabling its use in precise process design and control. In this model, factor values are entered in their original units, such as milliliters per hour, kilovolts, or centimeters, and the output is calculated on the actual scale. However, due to the dependence of the equation coefficients on the units and the range of each factor, this model cannot be used for direct comparison of the relative effects of the factors; a larger coefficient may simply result from a larger unit or wider range of that variable, rather than its true importance in the system. Therefore, this equation is primarily suitable for simulating experimental conditions, predicting system behavior at operational points, and engineering applications, whereas for statistical interpretation and comparison of relative factor effects, the equation expressed in coded factors should be used. This distinction plays a key role in the correct analysis of results obtained from experimental design methods such as RSM [30].

Final Equation of Diameter (nm) in Terms of Actual Factors = +1151.41025 -14.32958 CSO -138.23313 Pump rate -22.54500 Distance -28.93903 Voltage +0.229667 CSO * Distance -0.564444 Pump rate * Distance -2.32778 Pump rate * Voltage +0.522708 CSO^2 +42.51276 $Pump\ rate^2$ +0.579037 $Distance^2$ +0.813708 $Voltage^2$

The regression model based on coded factors demonstrated excellent agreement with the experimental data ($R^2 \approx 0.99$), indicating a significant influence of the studied variables on the diameter of CSO-loaded nanocarriers. Additionally, the low coefficient of variation (CV) reflects high reproducibility of the results and the adequate precision of the model.

Beyond analyzing the regression coefficients and their significance, assessing the adequacy and accuracy of the statistical model through residuals analysis plays a key role. Residuals represent the differences between observed values and those predicted by the model and indicate the portion of data variance that the model cannot explain. Therefore, a detailed examination of

residuals can provide valuable information about the validity, precision, and underlying assumptions of the model. One critical assumption in regression is the normality of residuals, as normality ensures the correctness of statistical tests, such as ANOVA, and confidence intervals. To evaluate this assumption, a normal probability plot is commonly and effectively used. In this plot, if the residuals approximately align along a straight line, it indicates a normal distribution, confirming the validity of the model. Furthermore, examining other plots, including residuals versus predicted values and residuals versus run order, can help identify non-random behavior, heteroscedasticity, or unexpected patterns in the data. These analyses complement the statistical evaluation of the model and can play a decisive role in detecting potential model deficiencies and improving it [31]. Fig 3 presents the normal probability plot of the residuals, showing that the residuals reasonably align along a straight line, indicating their normal distribution.

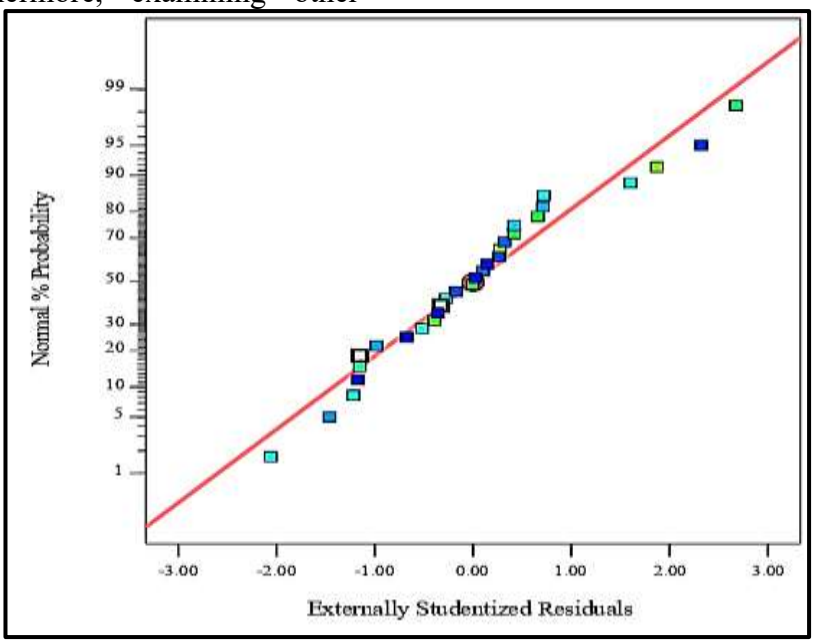

Fig 3. Normality plot of residuals

Fig 4 illustrates the response surface contour plots for the average diameter of the nanocarriers and the model desirability as a function of the interactions between the independent process variables. These plots provide a comprehensive visualization of the simultaneous effects of the factors on the morphological characteristics of the fibers. As observed from the response surface plots, both the nanocarrier diameter and the model desirability are directly and significantly influenced by all the examined variables, exhibiting fluctuations across different levels of the process parameters. Notably, extreme increases or decreases in the applied parameter levels lead to a considerable increase in the nanocarrier diameter.

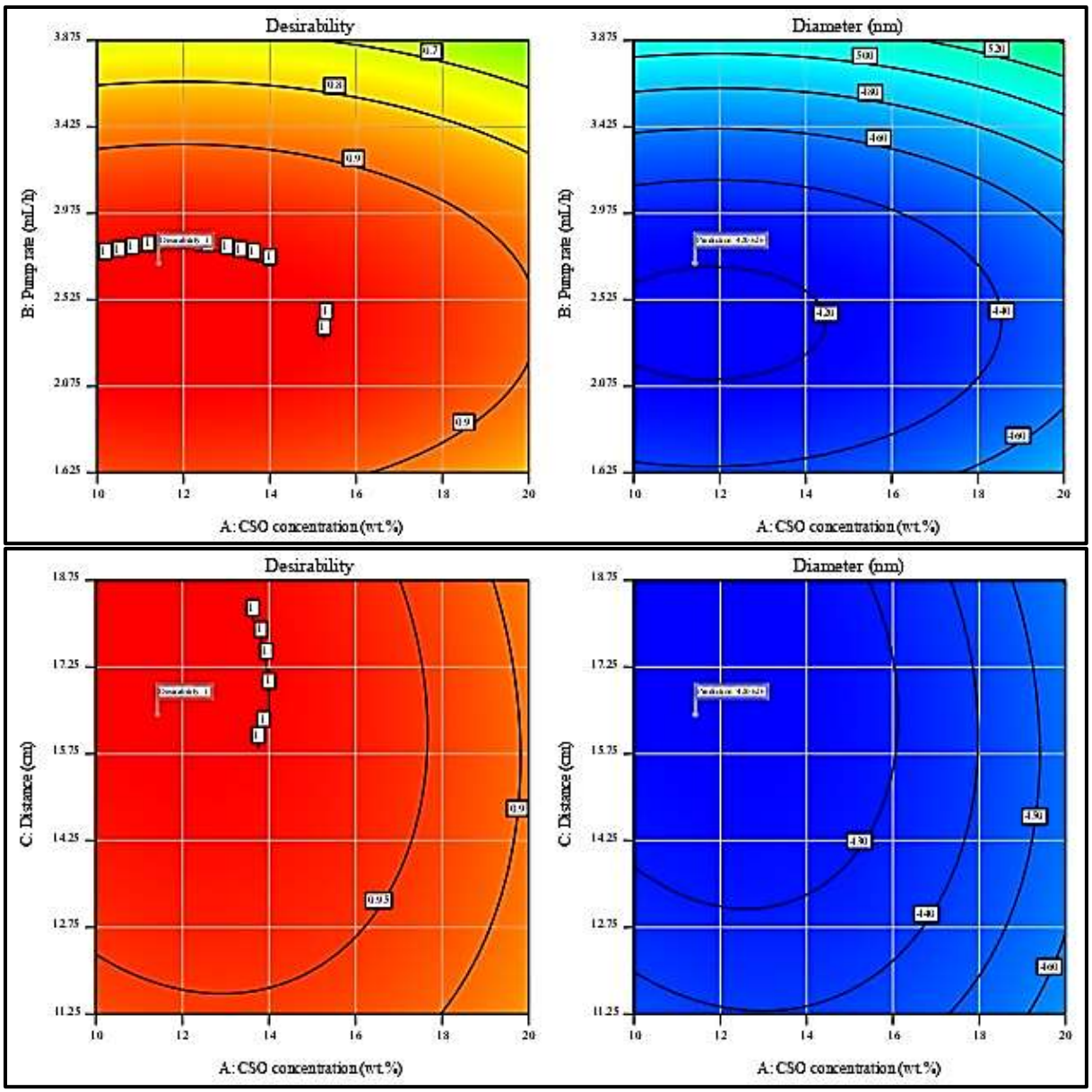
Desirability
Diameter (nm)
B: Pump rate (mL/h)
A: CSO concentration (wt.%)
C: Distance (cm)
A: CSO concentration (wt.%)
Desirability
Diameter (nm)
C: Distance (cm)
A: CSO concentration (wt.%)

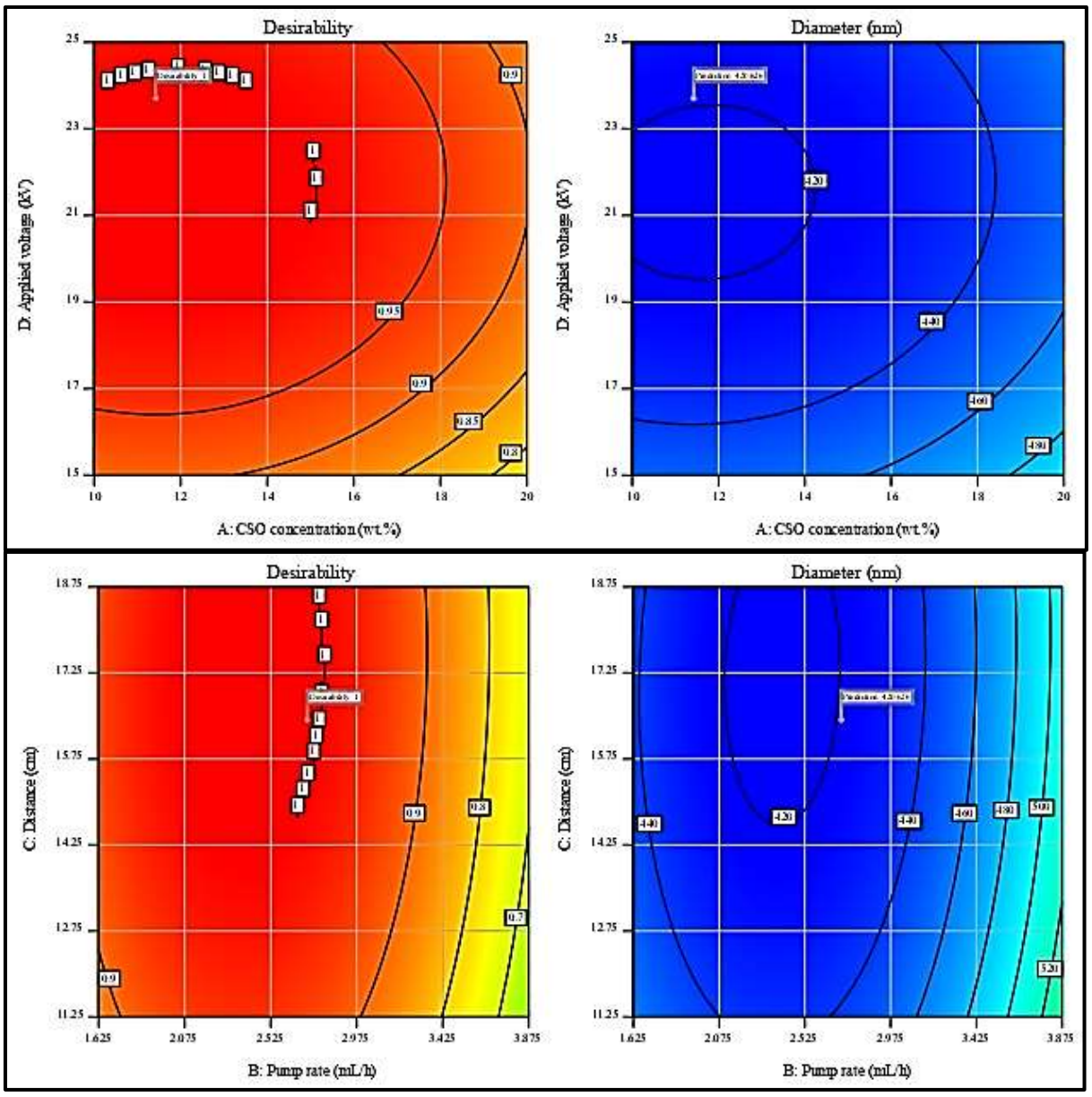
Desirability
Diameter (nm)
D: Applied voltage (kV)
A: CSO concentration (wt.%)
C: Distance (cm)
B: Pump rate (mL/h)

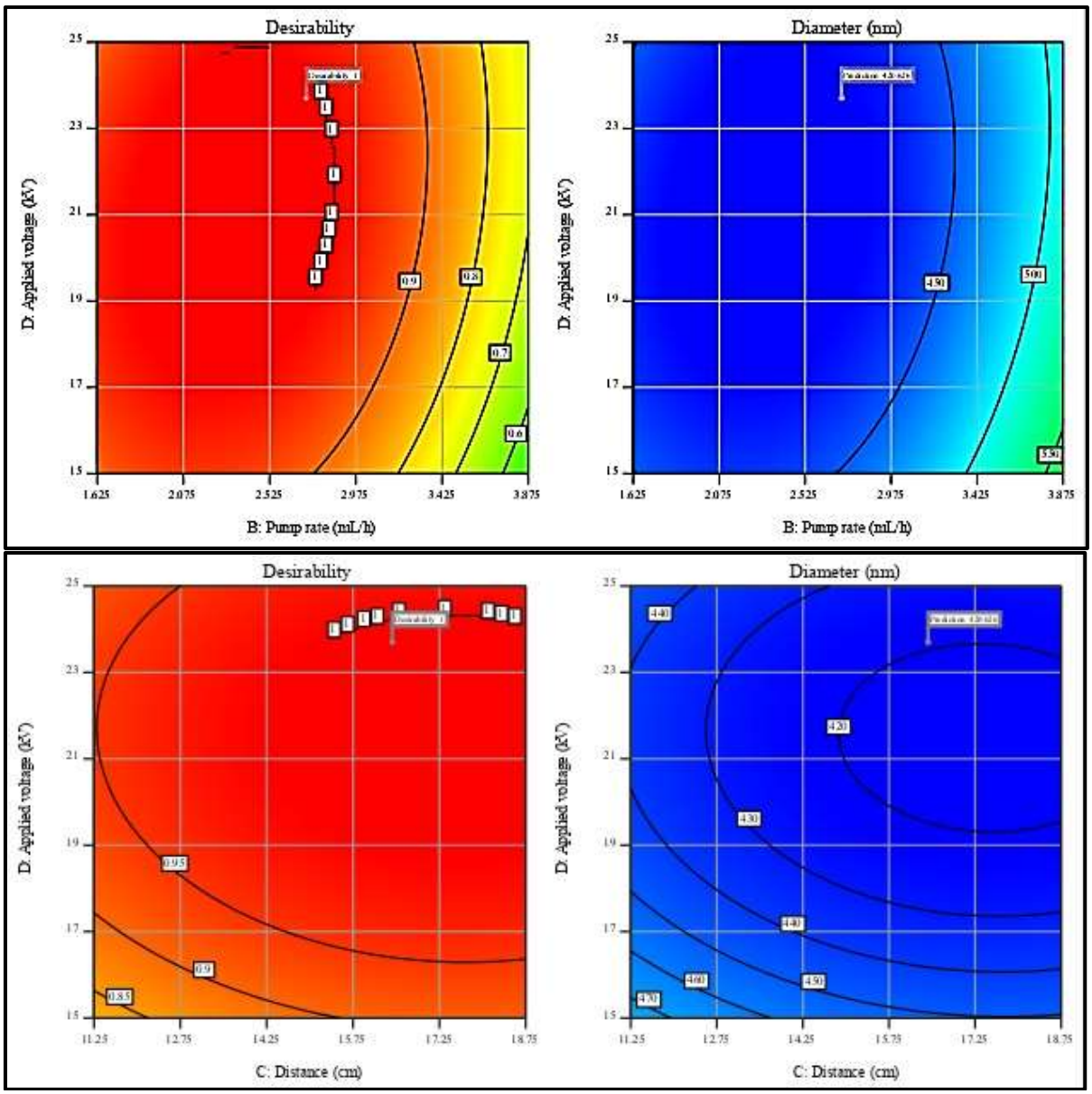

Fig 4. Contour plots of the interaction effect of variables on the diameter and desirability of the PVA-CSO nanocarrier

In the electrospinning process of PVA-CSO nanocarriers, the system behavior is influenced by complex interactions among the process variables, which can be analyzed using the RSM. The findings indicate that the amount of CSO, as a loaded component within the polymer matrix, exhibits a significant nonlinear behavior in interaction with other parameters. Specifically, at high CSO levels, the system becomes more sensitive to changes in the pump speed, meaning that any variation in flow rate produces larger changes in fiber diameter. This behavior can be attributed to the reduction in the effective viscosity of the polymer solution in the presence of the oil and the resulting changes in system rheology [32]. Furthermore, increasing CSO

concentration at all pump speeds leads to a uniform increase in fiber diameter, indicating the independent and positive role of this variable in fiber thickening.

In interaction with the needle-to-collector distance, the system is more sensitive at low CSO levels. In other words, at low oil concentrations, changes in the distance have a greater effect on fiber diameter, likely due to reduced effective electric stretching over longer distances and insufficient compensation by solution viscosity. Conversely, at longer distances, increasing CSO concentration has a more pronounced effect on diameter, suggesting that under these conditions, the rheological influence of the oil dominates jet behavior. The smallest interaction effect was observed at low CSO levels and long distances, likely due to the imbalance between electrical forces and solution viscosity [24].

Regarding applied voltage, the system is more sensitive to voltage changes at low CSO levels. This observation aligns with the studies by Ziyadi et al. (2021) and Hosseini et al. (2021), which reported that in the absence of oil loading, increasing voltage initially reduces jet diameter and subsequently leads to the formation of irregular (beaded) structures [33, 34]. In this study, at low voltages and low CSO concentrations, fiber diameter variations were more pronounced, whereas at high voltages, this sensitivity decreased, likely due to the dominance of electric forces over rheological effects. The minimum interactive effect was observed at low CSO levels and high voltages, indicating system saturation with respect to the electric field response [35].

For the pump speed–distance interaction, results indicate that at longer distances, variations in pump speed have a greater impact on fiber diameter, consistent with the findings of Theron et al. (2004), who showed that longer flight times reduce the opportunity for complete jet drying, resulting in droplet or bead formation [36]. In the present study, the highest interaction effect was observed at short distances and high pump speeds, suggesting that under these conditions, the imbalance between feed rate and drying time leads to increased diameter and structural heterogeneity [37].

Regarding the pump speed–voltage interaction, the system is more sensitive to voltage changes at high pump speeds. This behavior aligns with the reports of Rieger et al. (2016) and Li and Wang (2013), which indicated that simultaneous increases in flow rate and voltage can lead to larger fiber diameters due to higher polymer volume and reduced drying time [38, 39]. In this study, the greatest interactive effect was observed at high speeds and low voltages, indicating insufficient electric stretching to compensate for the increased jet mass.

Finally, the interaction between distance and voltage showed that at long distances, voltage variations have a stronger influence on diameter, which can be explained by the Taylor cone formation mechanism and jet stretching by the electric field [40]. At short distances and low voltages, the interactive effect reached its maximum, indicating that the system is at the edge of stability, where minor changes in parameters lead to significant morphological variations.

Since the optimization targeted only a single response (fiber diameter), the desirability function was normalized between 0 and 1. The trend of desirability closely followed the trend of fiber diameter, with values near the target

(optimal diameter) corresponding to desirability near 1 and values far from the target corresponding to desirability near 0. This consistency shows that in single-response problems, the desirability function serves merely as a quantitative tool for identifying the optimum region without altering system behavior.

Overall, the findings indicate that optimizing the electrospinning of PVA-CSO nanocarriers requires consideration of nonlinear interactions among the variables, particularly in the presence of oil components that alter the rheological and electrical behavior of the system. These results align with the studies of Topuz et al. (2021) on polymer concentration [32] and Theron et al. (2004) on surface charge density and flow rate [36], highlighting that designing electrospinning systems containing bioactive compounds necessitates multivariate modeling rather than simple univariate optimization. Optimization of independent variables and validation of the predicted outcomes are summarized in Table 4.

Table 4. Predicted optimal response conditions for PVA-CSO nanocarrier

Name	Goal	Lower Limit	Upper Limit	Predicted	Validated
A:CSO concentration (wt.%)	is in range	10	20	11.422	12
B:Pump rate (mL/h)	is in range	1.625	3.875	2.716	2.75
C:Distance (cm)	is in range	11.25	18.75	16.431	15
D:Applied voltage (kV)	is in range	15	25	23.702	25
Diameter (nm)	minimize	422.9	726.2	420.626	422.8

To investigate the microstructure of the PVA-CSO nanocarriers, Fig 5 presents the SEM image of the electrospun sample prepared under optimized conditions.

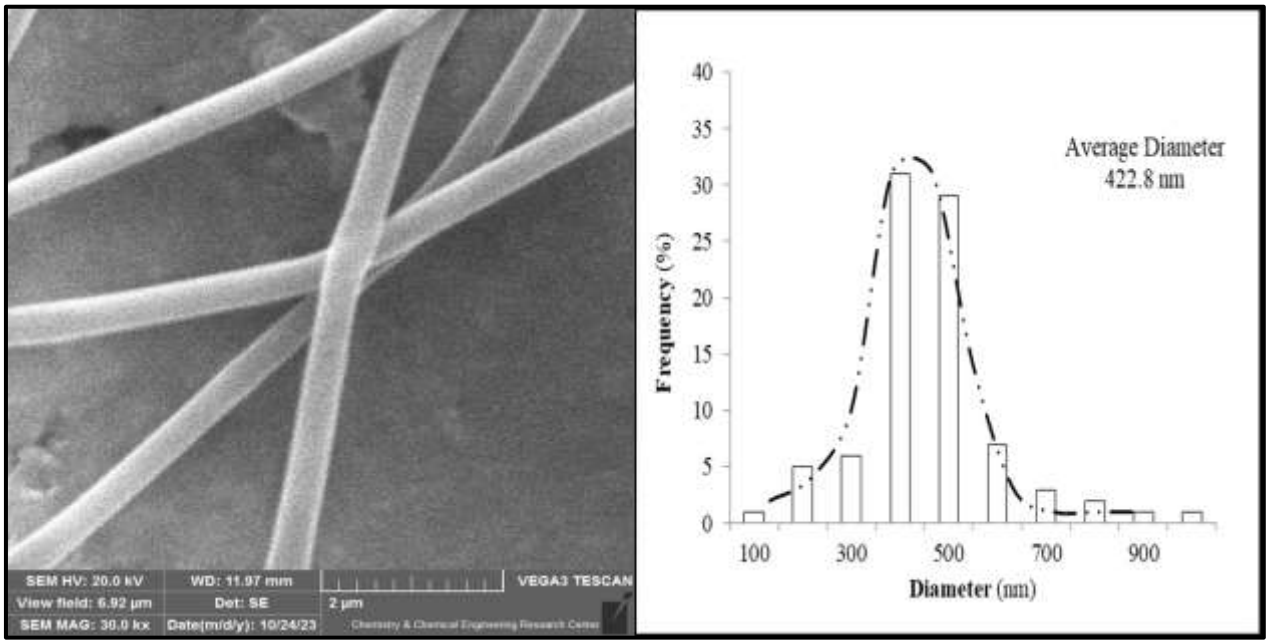

Fig 5. SEM image and diameter distribution histogram of PVA-CSO nanocarrier in optimal electrospinning condition

Based on the SEM results, it can be concluded that the obtained PVA-CSO nanocarriers, with an average diameter of approximately 420 nm, exhibit acceptable uniformity. The normal distribution of the formed nanocarriers is a key factor confirming the reliability of the process [41]. SEM images indicated that the nanocarriers were uniform and bead-free. No significant aggregation was observed, further confirming the optimality of the electrospinning parameters. The diameter distribution of the nanocarriers was approximately normal, with around 60% of the nanofibers falling within the 400–500 nm range, which is considered desirable.

4. Conclusion

This study aimed to optimize the electrospinning conditions for PVA-based nanocarriers loaded with CSO. Using RSM and statistical analysis, the effects of process variables on the diameter and morphology of the nanocarriers were evaluated. The results demonstrated that PVA polymer exhibits high compatibility with electrospinning conditions and can serve as a suitable matrix for encapsulating plant oils and extracts, including CSO. Moreover, the produced nanocarriers, with the capability of controlled release of bioactive compounds, hold significant potential for enhancing the performance of active packaging and smart sensors in the food industry. These findings underscore the effectiveness of the proposed optimization approach for the development of practical nanocarrier systems in food applications.

Funding

The author declares that he / she has not received any funding.

Author Contributions

All activities were carried out by the author.

Competing Interests

The author confirms that he / she has no financial conflicts of interest or competing interests in this study.

Acknowledgements

The authors would like to express their sincere gratitude to the Vice-chancellor for Research and Technology of Agricultural Sciences and Natural Resources University of Khuzestan for supporting this study (1403.38).

5-References

[1] Khaledi, S., et al., *An innovative anti-radical electrospun nanofiber patch infused with microwave-roasted polyphenol-rich Camelina (Camelina sativa L.) seed oil as controlled release food packaging: S. Khaledi et. al.* Journal of Food Measurement and Characterization, 2025: p. 1-17.

[2] Emam-Djomeh, Z., M. Ekrami, and A. Ekrami, *Design and use of hydrogels for food component encapsulation.* Materials Science and Engineering in Food Product Development, 2023: p. 211-226.

[3] Ekrami, M., et al., *Next-Generation Smart and Safe Foods: Artificial Intelligence-Driven Strategies for 4D Food Pre-Printing Challenges.* Trends in Food Science & Technology, 2025: p. 105317.

[4] Farahmand, E., et al., *Polymethacrylate coated electrospun chitosan/PEO nanofibers loaded with thyme essential oil: a newfound potential for antimicrobial food packaging.* Journal of Food and Bioprocess Engineering, 2023. **6**(2): p. 8-16.

[5] Ekrami, M., et al., *Nanotechnology-based formulation for alternative medicines and*

natural products: an introduction with clinical studies. 2022.
[6] Pires, J.B., et al., *Essential oil encapsulation by electrospinning and electrospraying using food proteins: A review.* Food Research International, 2023. **170**: p. 112970.
[7] Mondor, M. and A.J. Hernández-Álvarez, *Camelina sativa composition, attributes, and applications: A review.* European Journal of Lipid Science and Technology, 2022. **124**(3): p. 2100035.
[8] Zanetti, F., et al., *Camelina, an ancient oilseed crop actively contributing to the rural renaissance in Europe. A review.* Agronomy for Sustainable Development, 2021. **41**(1): p. 2.
[9] Ghobadi, R., et al., *Nutritional properties and benefits of camelina oil and meal.* Agrotechniques in Industrial Crops, 2021. **1**(2): p. 71-76.
[10] Sheybani, F., et al., *Application of nanostructured lipid carriers containing α-tocopherol for oxidative stability enhancement of camelina oil.* Industrial Crops and Products, 2023. **202**: p. 117007.
[11] Ekrami, M., et al., *Food-based polymers for encapsulation and delivery of bioactive compounds.* 2022.
[12] Taheri-Shakib, J. and A. Kantzas, *A comprehensive review of microwave application on the oil shale: Prospects for shale oil production.* Fuel, 2021. **305**: p. 121519.
[13] Walayat, N., et al., *Oxidative stability, quality, and bioactive compounds of oils obtained by ultrasound and microwave-assisted oil extraction.* Critical Reviews in Food Science and Nutrition, 2024. **64**(27): p. 9974-9991.
[14] Asadzadeh, R., et al., *Optimization of the electrospinning process of hybrid nanocarrier based on mung bean (Vigna radiate L.) protein/poly (vinyl alcohol).* Food Engineering Research, 2024. **23**(1): p. 165-182.
[15] Tehrani, E. and S. Amiri, *Synthesis and characterization PVA electro-spun nanofibers containing encapsulated vitamin C in chitosan microspheres* .The Journal of the Textile Institute, 2022. **113**(2): p. 212-223.
[16] de Jesus Silva, J., et al., *Encapsulation of açaí (Euterpe oleracea) pulp with whey protein isolate by spray-drying: An optimization study using response surface methodology (RSM).* Food and Humanity, 2023. **1**: p. 1539-1546.
[17] Mahdavi, Z., et al., *Application of RSM-CCD methodology and image J. for modeling and optimization of orchid protocorm encapsulation.* Heliyon, 2025. **11**.(٤)
[18] Rezaei, S., et al., *Qualitative and quantitative assessment of extracted oil from Camelina sativa seed treated by dielectric-barrier discharge cold plasma.* Contributions to Plasma Physics, 2020. **60**(9): p. e202000032.
[19] Zeinali, T., et al., *Fabrication and characterization of jujube extract-loaded electrospun polyvinyl alcohol nanofiber for strawberry preservation.* Food science & nutrition, 2021. **9**(11): p. 6353-6361.
[20] Ekrami, M., et al., *pH-Responsive Color Indicator of Saffron (Crocus sativus L.) Anthocyanin-Activated Salep Mucilage Edible Film for Real-Time Monitoring of Fish Fillet Freshness.* Chemistry, 2022. **4**(4): p. 1360-1381.
[21] Senthilkumar, T., S. Chattopadhyay, and L.R. Miranda, *Optimization of activated carbon preparation from pomegranate peel (Punica granatum peel) using RSM.* Chemical engineering communications, 2017. **204**(2): p. 238-248.
[22] Chinnappan, B.A., et al., *Electrospinning of biomedical nanofibers/nanomembranes: Effects of process parameters.* Polymers, 2022. **14**(18): p. 3719.
[23] Ahmadi Bonakdar, M. and D. Rodrigue, *Electrospinning :Processes, structures, and materials.* Macromol, 2024. **4**(1): p. 58-103.
[24] Ji, D., et al., *Electrospinning of nanofibres.* Nature Reviews Methods Primers, 2024. **4**(1): p. 1.
[25] Keirouz, A., et al., *The history of electrospinning: past, present, and future developments.* Advanced Materials Technologies, 2023. **8**(11): p. 2201723.
[26] Yang, J. and L. Xu, *Electrospun nanofiber membranes with various structures for wound dressing.* Materials, 2023. **16**(17): p. 6021.
[27] Li, L., et al., *Electrospun fibers control drug delivery for tissue regeneration and cancer therapy.* Advanced Fiber Materials, 2022. **4**(6): p. 1375-1413.

[28] Han, W., et al., *A review: Current status and emerging developments on natural polymer-based electrospun fibers.* Macromolecular Rapid Communications, 2022. **43**(21): p. 2200456.
[29] Lenth, R.V., *Response-surface methods in R, using rsm.* Journal of statistical Software, 2010. **32**: p. 1-17.
[30] Baş, D. and İ.H. Boyacı, *Modeling and optimization I: Usability of response surface methodology.* Journal of food engineering, 2007. **78**(3): p. 836-845.
[31] Khuri, A.I. and S. Mukhopadhyay, *Response surface methodology.* Wiley Interdisciplinary Reviews: Computational Statistics, 2010. **2**(2): p. 128-149.
[32] Topuz, F., et al., *Nanofiber engineering of microporous polyimides through electrospinning: Influence of electrospinning parameters and salt addition.* Materials & Design, 2021. **198**: p. 109280.
[33] Hosseini, F., et al., *Encapsulation of rosemary essential oil in zein by electrospinning technique.* Journal of Food Science, 2021. **86**(9): p. 4070-4086.
[34] Ziyadi, H., et al., *An investigation of factors affecting the electrospinning of poly (vinyl alcohol)/kefiran composite nanofibers.* Advanced Composites and Hybrid Materials, 2021. **4**: p. 768-779.
[35] Cho, Y., et al ,.*Electrospinning and nanofiber technology: fundamentals, innovations, and applications.* Advanced Materials, 2025. **37**(28): p. 2500162.
[35] Theron, S., E. Zussman, and A. Yarin, *Experimental investigation of the governing parameters in the electrospinning of polymer solutions.* Polymer, 2004. **45**(6): p. 2017-2030.
[36] Lian, S., D. Lamprou, and M. Zhao, *Electrospinning technologies for the delivery of Biopharmaceuticals: Current status and future trends.* International Journal of Pharmaceutics, 2024. **651**: p. 1.٢٣٦٤١
[37] Li, Z., et al., *Effects of working parameters on electrospinning.* One-dimensional nanostructures: Electrospinning technique and unique nanofibers, 2013: p. 15-28.
[38] Rieger, K.A., N.P. Birch, and J.D. Schiffman, *Electrospinning chitosan/poly*) *ethylene oxide) solutions with essential oils: Correlating solution rheology to nanofiber formation.* Carbohydrate polymers, 2016. **139**: p. 131-138.
[39] Shabani, A., et al., *Electrospinning Technology, Machine Learning, and Control Approaches: A Review.* Advanced Engineering Materials, 2025. **27**(7): p. 2401353.
[40] Sencadas, V., et al., *Determination of the parameters affecting electrospun chitosan fiber size distribution and morphology.* Carbohydrate Polymers, 2012. **87**(2): p. 1295-1301.

مجله علوم و صنایع غذایی ایران

سایت مجله: www.fsct.modares.ac.ir

مقاله علمی_پژوهشی

بهینه‌سازی فرایند الکتروریسی نانوحامل پلی وینیل الکل حاوی روغن دانه کاملینا (*Camelina sativa* L.) برشته‌شده با مایکروویو

ساناز خالدی[۱]، نفیسه جهانبخشیان[۲*]، زهرا امام جمعه [۳]، صدیقه سلیمانی فرد[۴]، زهرا بیگ محمدی[۱]

۱- گروه علوم و مهندسی صنایع غذایی، واحد تهران شمال، دانشگاه آزاد اسلامی، تهران، ایران

۲- گروه علوم و مهندسی صنایع غذایی، واحد شهرکرد، دانشگاه آزاد اسلامی، شهرکرد، ایران

۳- گروه علوم، فناوری و مهندسی صنایع غذایی دانشکده فنی و مهندسی کشاورزی پردیس کشاورزی دانشگاه تهران، کرج، ایران

۴- گروه علوم و مهندسی صنایع غذایی، دانشکده کشاورزی، دانشگاه زابل، زابل، ایران

اطلاعات مقاله

تاریخ های مقاله :

تاریخ دریافت: ۱۴۰۴/۰۵/۰۶

تاریخ داوری: ۱۴۰۴/۰۷/۰۸

تاریخ پذیرش: ۱۴۰۴/۰۷/۱۵

کلمات کلیدی:

نانوحامل،

الکتروریسی،

روغن کاملینا،

طراحی سطح پاسخ،

برشته‌شده

DOI: 10.48311/fsct.2026.84077.0

* مسئول مکاتبات:

njahanbakhshian@iau.ac.ir

چکیده

نانوحامل‌ها به‌عنوان سامانه‌های نوین رهایش ترکیبات زیست‌فعال، نقش مهمی در افزایش پایداری، بهبود کارایی و توسعه کاربردهای نوآورانه در صنایع غذایی و بسته‌بندی ایفا می‌کنند .در این پژوهش، تولید و بهینه‌سازی نانوحامل‌های زیست‌سازگار بر پایه پلی‌وینیل الکل حاوی روغن دانه کاملینا برشته‌شده شده با مایکروویو، به‌منظور کاربرد در بسته‌بندی هوشمند مواد غذایی بررسی شد. از روش الکتروریسی و طراحی آزمایش سطح پاسخ بر پایه طرح مرکزی مرکب برای بررسی تأثیر متغیرهایی چون مقدار روغن (۲۵-۵ درصد وزنی)، ولتاژ (۳۰-۱۰ کیلوولت)، فاصله سوزن تا جمع کننده (۲۲/۵-۷/۵ سانتی متر) و سرعت پمپ (۵-۰/۵ میلی لیتر بر ساعت) بر قطر نانوحامل‌ها استفاده شد. مدل رگرسیون برازش‌شده همبستگی بالایی بین متغیرها و پاسخ (R^2=۰/۹۹۸) نشان داد. نتایج آنالیز واریانس و نمودار پارتو بیانگر تأثیر معنی‌دار سرعت پمپ و مقدار روغن بر قطر نانوحامل بود. این نانوحامل‌ها با قابلیت انکپسولاسیون ترکیبات زیست‌فعال، می‌توانند در طراحی سیستم‌های بسته‌بندی فعال و حسگرهای هوشمند مواد غذایی مورد استفاده قرار گیرند.